J. of Supercritical Fluids 158 (2020) 104748

Contents lists available at ScienceDirect

The Journal of Supercritical Fluids

journal homepage: www.elsevier.com/locate/supflu

Paramagnetic bioactives encapsulated in poly(D,L-lactide) microparticules: Spatial distribution and *in vitro* release kinetics

Golubeva E.N.[a], Chumakova N.A.[a,*], Kuzin S.V.[a], Grigoriev I.A.[c], Kalai T.[d], Korotkevich A.A.[a], Bogorodsky S.E.[b], Krotova L.I.[b], Popov V.K.[b], Lunin V.V.[a]

[a] Lomonosov Moscow State University, Department of Chemistry, Leninskie Gory 1-3, Moscow 119991, Russia
[b] Institute of Photon Technologies of Federal Scientific Research Centre "Crystallography and Photonics" Russian Academy of Sciences, Pionerskaya 2, Troitsk, Moscow, 108840, Russia
[c] Vorozhtsov Novosibirsk Institute of Organic Chemistry Siberian Branch of the Russian Academy of Sciences, Lavrentiev Ave., 9, Novosibirsk, 630090, Russia
[d] Institute of Organic and Medicinal Chemistry, University of Pécs, Medical School, Szigeti St. 12, H-7624, Pécs, Hungary

HIGHLIGHTS

- PGSS was used for fabrication of poly(D,L-lactide) microparticles impregnated with paramagnetic bioactives.
- EPR spectroscopy revealed homogeneous spatial distribution for the most of the dopants.
- Quantitative EPR was applied for estimation of regularities of *in vitro* dopant release.

GRAPHICAL ABSTRACT

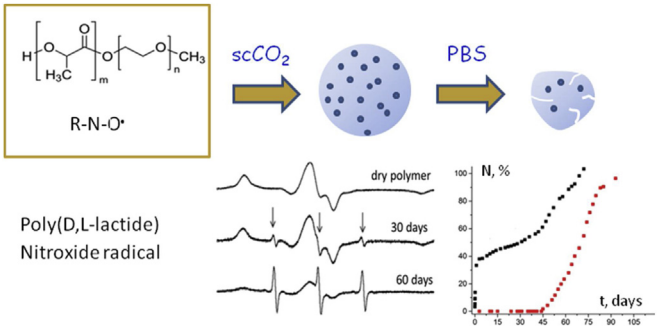

ARTICLE INFO

Article history:
Received 5 December 2019
Received in revised form
26 December 2019
Accepted 28 December 2019
Available online 8 January 2020

Keywords:
Release kinetics
Paramagnetic bioactives
Poly(D,L-lactide)
Supercritical fluid micronization and impregnation
Electron paramagnetic resonance

ABSTRACT

Poly(D,L-lactide) microparticles impregnated with a number of bioactive paramagnetic compounds have been fabricated using two SCF techniques: 1). PGSS (Particles from Gas Saturated Solution) and 2). polymer plasticization and swelling by supercritical carbon dioxide followed by its cryomilling. Electron paramagnetic resonance (EPR) spectroscopy manifested homogeneous spatial distribution for the most of these substances encapsulated into the polymer. Irreversible relaxation processes in the prepared polymer structures and formulations were not observed. The qualitative difference in the release kinetics of paramagnetic molecules of different structure from the polymer microparticles into the phosphate-buffered saline (PBS, pH = 7.4) was demonstrated. pH-sensitive ATI spin probe proved the decrease (up to $\leq$ 4.5) of local pH inside the microparticles during the first 9 days after its immersion in PBS.

1. Introduction

Nowadays, biodegradable polymer microparticles impregnated with biologically active compounds are considered as a perspective components of dosage forms for drug delivery and controlled drug release [1–5]. The main criteria in selecting polymer materials for

* Corresponding author.
E-mail address: harmonic2011@yandex.ru (N.A. Chumakova).

https://doi.org/10.1016/j.supflu.2019.104748
0896-8446/

this purpose are: the biocompatibility, an appropriate degradation rate, ability for sustained drugs release and low cost straightforward production [5]. Aliphatic polyesters, such as polylactides, polyglycolide and their copolymers - polylactide-co-glycolides (PLGA) generally satisfy the major part of these demands. They are readily hydrolyzed in the body to the respective monomers and oligomers that are soluble in aqueous media and can be easily removed from the organism [1].

Supercritical fluid (SCF) technologies usually based on supercritical carbon dioxide (sc–CO_2, critical temperature T_{cr} =304 K, critical pressure P_{cr} =7.4 MPa) are the promising R&D methodology in modern pharmacy. They enable effective fabrication of biodegradable polymer scaffolds or microparticles impregnated with bioactive agents without any use of toxic organic solvents and high (above 313 K) temperatures [2,6–9]. PGSS (Particles from Gas Saturated Solution) is one of such techniques where polymer, plasticized by sc–CO_2, thoroughly mixed with dissolved (or previously micronized) bioactive substances, is expanding through a nozzle into a low-pressure (usually, atmospheric) vessel forming impregnated polymer microcapsules [2,6,10].

Degradation of the aliphatic polyesters due to their hydrolysis is one of the major factors governing the release of bioactive agents into the aqueous environment. This process is complicated by autocatalytic action of the reaction products lowering pH of the medium and facilitating bulk erosion [11–15]. Moreover, diffusion of the polymer degradation products and encapsulated drug outside the polymeric matrix (or microparticles) is influenced by its shape and swelling characteristics [11,12,16]. The nature of bioactive agents and character of their spatial distribution in polymer matrix also govern the release features. Hydrophilic drugs promote water transport into the matrix and thereby accelerate its degradation. Hydrophobic drugs usually make an opposite effect [11]. Acidic substances act as catalysts of ester bond cleavage [17–19]. Basic dopants can neutralize carboxyl end groups reducing the polymer degradation rate, but are themselves the catalysts of hydrolysis [11,20]. Irregular spatial distribution of drugs may result in their uneven release [21].

Electron paramagnetic resonance (EPR) method allows observing the molecules containing unpaired electrons (paramagnetic molecules); all other substances are invisible in EPR. The spin probing technique, based on adding of small quantity of paramagnetic dopants into non-paramagnetic matrix, provides remarkable possibilities to study the intrinsic features (free volume, polymer chains mobility, polarity, pH, etc.) of a wide range of polymeric materials at microscopic level, as well, as spatial distribution of paramagnetic molecules throughout the impregnated matrix [22]. Nitroxide radicals are the most often applied spin probes due to the high sensitivity of their EPR spectra shape to the rotation velocity of paramagnetic molecules caused by high anisotropy of hyperfine coupling (hfc) tensor [22–24]. The majority of nitroxide radicals are not only low-toxic [25], but also have anti-cancer and antioxidant properties [25–28]. According to recent literature data, in many cases the presence of a nitroxide fragment in the molecule of a biologically active substance leads to a positive synergistic effect [29].

In the present paper, we demonstrate the advantages of spin probe and spin label approach for the study of bioactives spatial distribution in poly(D,L-lactide) microparticles fabricated by PGSS technique, as well as the main peculiarities of the *in vitro* model drug release from the polymer particles to phosphate-buffered saline (PBS). The standard nitroxide radical TEMPOL, pH-sensitive radical ATI, and spin-labeled biologically active substances dihydroquercetin (DHQ), α-tocopheryl succinate (α-TOS), and diclofenac (DCF) were chosen as model paramagnetic dopants (see Fig. 1). DHQ is a natural flavonoid with powerful antioxidant, hepatoprotective, anti-inflammatory and antihistamine properties [30,31]. α-Tocopherol (vitamin E) is well-known antioxidant [32,33]. Its derivatives, among which the lead compound is α-tocopheryl succinate, a mitochondrial-targeted antitumor drug induce apoptosis of cancer cells at concentrations that are non-toxic for healthy cells and tissues, inhibit cancer cell proliferation, and enhance the action of other anticancer drugs reducing their toxicity to normal cells [34]. α-TOS containing in a single molecule pharmacologically active succinyl, nitroxide and chromane fragments is perspective as hybrid polyfunctional compound [35]. Diclofenac is widely used as anti-inflammatory, analgesic and antipyretic agent [36,29]. It is necessary to note that DCF (acid form or sodium salt) and TCF are predominantly encapsulated in polylactides and polylactoglycolides by oil-in-water emulsion-solvent evaporation method [37–40]. In [41] diclofenac sodium was introduced into polylactoglycolide using SCF technique.

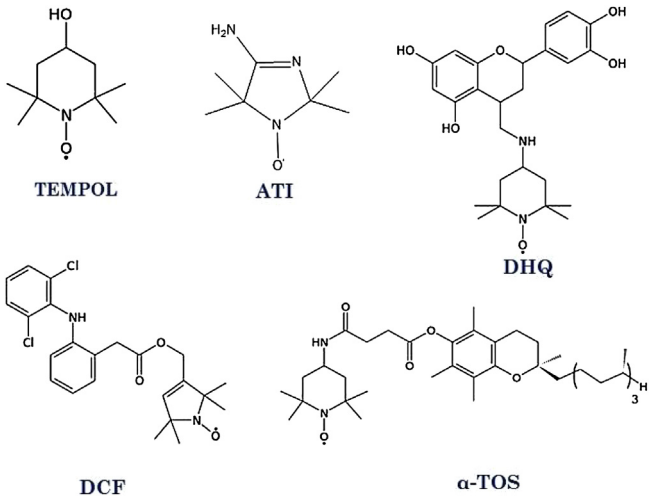

Fig. 1. The structures of paramagnetic compounds.

2. Experimental

2.1. Materials and methods

Stable nitroxide radical TEMPOL was purchased from Sigma-Aldrich. pH-sensitive radical ATI was synthesized as described elsewhere [42]. Synthesis of spin-labeled bioactive agents dihydroquercetin (DHQ) and α-tocopheryl succinate (α-TOS) were described in [43] and [34], respectively. Synthesis of 1-oxyl-2,2,5,5-tetramethyl-2,5-dihydro-1H-pyrrol-3-yl)methyl-(2-((2,6-dichlorophenyl)amino)phenyl)acetate Radical (DCF) was carried out as follows.

To a stirred solution of sodium salt of diclofenac **1** (954 mg, 3.0 mmol) in anhydr. DMF (7 mL) allylic bromide **2** (770 mg, 3.3 mmol) dissolved in anhydr. DMF (3 mL) was added dropwise at 0 °C. After stirring the solution at r. t. overnight, the solvent was evaporated in vacuo, the residue was dissolved in EtOAc (30 mL), washed with water (10 mL), the organic phase was separated, dried ($MgSO_4$), filtered and evaporated. The residue was purified by flash column chromatography (hexane/Et_2O) to give the title compound 1.12 g (84 %) as a yellow solid, mp 75–77 °C, R_f: 0.52 (hexane/Et_2O, 1:1).

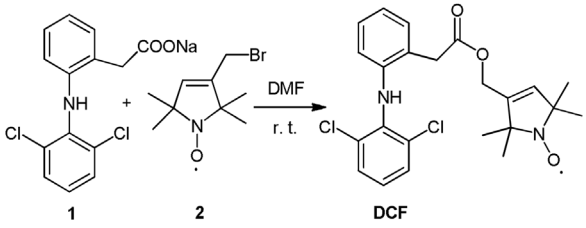

IR: 3336, 2972, 1719, 1604, 1585, 1564 cm^{-1}.

MS (EI): *m*/z (%) = 447/449/451 (11/7/1, $[M]^+$), 417 (1), 295/297/299 (51/31/5), 214 (100), 138 (46).

Anal. calcd. for $C_{23}H_{25}Cl_2N_2O_3$ C, 61.61; H, 5.62; N, 6.25 found: C, 61.54; H, 5.50; N, 6.11.

Melting points were determined with a Boetius micro-melting point apparatus. Elemental analyses (C, H, N, and S) were performed with a Fisons EA 1110 CHNS elemental analyzer. Mass spectra were recorded on a ThermoQuest automass Multi spectrometer. IR spectra were recorded with a Bruker Alpha FT-IR instrument with ATR support (ZnSe plate). Flash column chromatography was performed on Merck Kieselgel 60 (0.040-0.063 mm). TLC was run on Merck Kieselgel 60 F_{254}. Compound **2** was prepared as described previously [44]. Diclofenac sodium salt was purchased from Aldrich.

Toluene (Component Reactive) was distilled over metallic sodium. Phosphate-buffered saline (PBS) tablets were purchased from "Puschinskiye Laboratorii". The PBS solution was prepared by dissolving one tablet in 200 mL of distilled water. All chemicals were used as received, unless otherwise stated.

Medical grade poly(D,L-lactide) PURASORB® PDL02 (Purac Biochem bv, Netherlands) with inherent viscosity C = 0.2 g/dl was used as a raw polymer material. Chemically pure carbon dioxide (99.998 % grade, NIIKM Ltd., Russia) was applied as a plasticizing and spraying agent.

2.2. SCF fabrication of polylactide microparticles impregnated with paramagnetic substances

PGSS, in our opinion, is the most promising option for using SCF technologies to micronize a number of insoluble in sc–CO_2 amorphous polymers and encapsulate various biologically active molecules (e.g., pharmaceuticals) into the resulting microparticles. This method is based on specific interaction of high pressure CO_2 with polymer leading to an increase in polymer chain segmental mobility, which in turn, reduces the glass transition temperature T_g or melting point of the polymer [45]. The degree of this decrease depends on the amount of carbon dioxide dissolved (or sorbed) in the polymer [46]. At the same time spraying of plasticized, under pressure of fluid (in a sub - or supercritical state) and saturated to a certain level, polymer in the receiver at low (usually atmospheric pressure) leads to the microparticles formation [10].

Fig. 2 shows a schematic diagram of our (designed and produced at IPT FSRC «Crystallography and Photonics» RAS) laboratory set-up for the fine dispersed polymer powder fabrication using PGSS technique. PGSS set-up consists of the following main components: a high-pressure compressor, an autoclave comprising injection, spraying, drying, and microparticle collecting systems. The NWA PM 101 compressor from NWA GmbH (Laurach, Germany) allows working with various gases (butane, CO_2, propane) and injecting them into an autoclave to a pressure of 40 MPa. The main advantage of the compressor used is the ability to automatically maintain the required pressure in the autoclave. This allows it to be used for pumping supercritical fluids in stationary conditions or for working with them in continuous cycle regime. In an autoclave (allowing operation at pressures up to 40 MPa and temperatures up to 363 K) with an internal volume of 75 mL polymer plasticization in sc–CO_2 and mechanical mixing (using a magnetic stirrer) of the initial components take place. To seal it, a clamp with EPDM O Ring 70 Sn sealing rings from Brammer NDC UK Ltd (London, England) is used. The autoclave is equipped with a thermocouples, safety valve, pressure gauge and heater.

The injection system of SCF plasticized polymer is equipped with 3 interchangeable nozzles and provides the SCF mixture spraying into the low pressure chamber. To ensure pulse-periodic operation of the nozzle (pulse duration did not exceed 1 s), an MS-151 DA HT valve from Swagelok (USA), equipped with a pneumatic actuator, is used. Nozzles made of stainless steel 316 SS are interchangeable blocks with outlets with internal diameters of 300, 500 and 900 microns. Additionally, the injection system and the valve are equipped with an external heating element and a thermostatic winding to maintain a constant temperature. The solution injection system is also equipped with a thermocouple and a heat-resistant rubber seal.

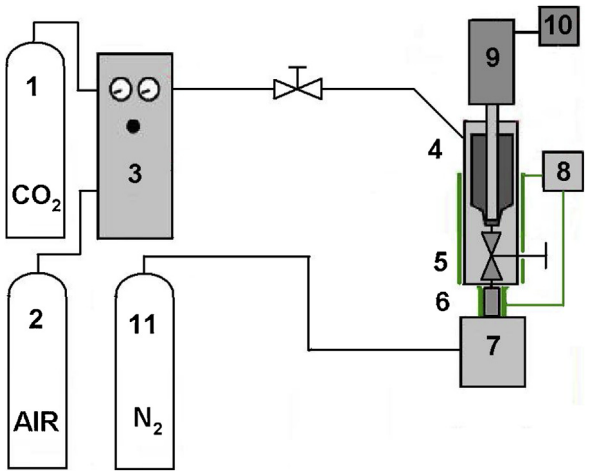

Fig. 2. Schematic diagram of PGSS set-up. 1 –CO_2 cylinder, 2 - air cylinder for compressor operation, 3 - compressor, 4 - high-pressure reactor (autoclave), 5 - outlet valve with pneumatic actuator, 6 - injection system, 7 - particle spraying chamber, 8 - heating and thermal stabilization controllers; 9 - magnetic stirrer; 10 - power supply and control unit for magnetic stirrer drive; 11 - nitrogen cylinder for low-pressure particle spraying chamber.

The injection system is connected to a 1000 mL low pressure particle spraying chamber. The main advantage of using such a chamber is the ability to change the morphology and size of the formed particles using an inert gas flow. When the pneumatic valve was opened, the plasticized polymer mixture was sprayed into the chamber through the injection system. During spraying, an inert gas (in our case, nitrogen) is fed into the chamber, the jet of which "inflates" the flow of the formed polymer particles, preventing their agglomeration.

SCF micronization of initial PDL02 and its simultaneous impregnation with paramagnetic molecules was carried out as follows. TEMPOL, α-TOS, DHQ and DCF were dissolved in ethyl alcohol (1 mg, 0,7 mg, 2 mg and 1 mg in 1 mL of ethanol, correspondently) before mixing with polymer. ATI was used without any pre-treatment. The amount of dopant was chosen in such a way the average distance between paramagnetic centers in polymer matrix was not shorter then 100 Å to avoid broadening of the EPR spectra as a result of the dipole – dipole interaction of radicals. Then stable radicals or their ethanol solutions were mixed with preliminary cryomilled (using dry ice at −78 °C) by rotary mill PDL02 powder (50÷200 μm). The mixture was dried in air for 30 min and placed inside a 75 mL high-pressure reactor. The reactor was filled with carbon dioxide. The temperature of the reactor was maintained at 313 K, the temperature of the nozzles was 343 K. The pressure of CO_2 was maintained at 10 MPa. The contents of the reactor were thoroughly mixed using a magnetic mixer at a speed of 20 rpm. The system was kept under these conditions for 120 min. During this time, complete plasticization of the polymer and its mixing with the paramagnetic compound occurred. Two different techniques were applied to prepare the micronized polymer. In the first case, the pressure was released from the chamber for 20 s, after which the resulting foamed sample was removed from the reactor, mixed with dry ice and ground by rotary mill (Cryomilling). In the

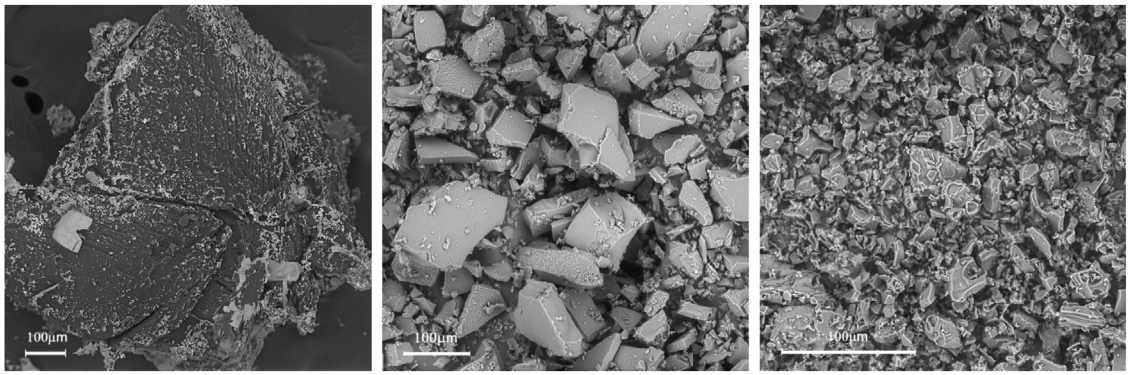

Fig. 3. SEM images of initial TEMPOL crystal (left), PDL02/TEMPOL microparticles fabricated by Cryomilling (middle) and by PGSS (right).

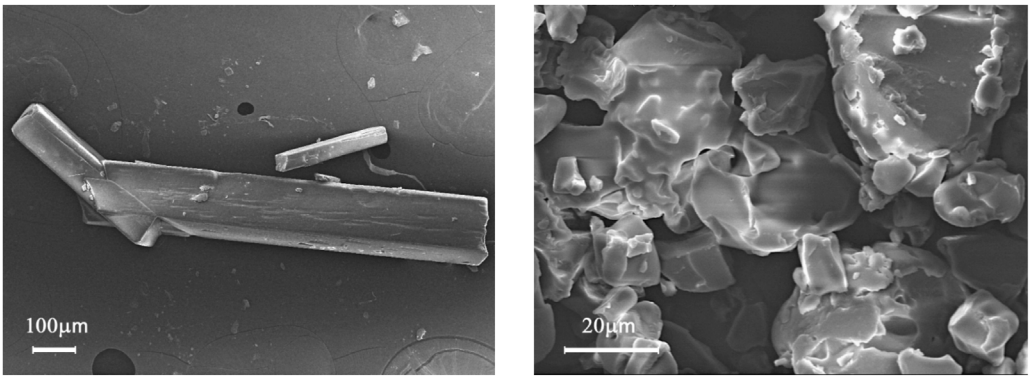

Fig. 4. SEM images of initial ATI crystal (left) and PDL02/ATI microparticles fabricated by PGSS (right).

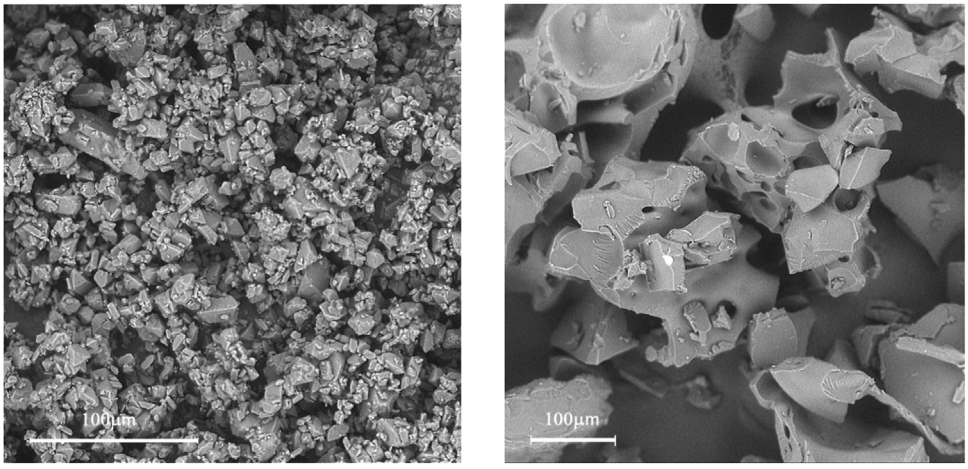

Fig. 5. SEM images of initial DCF crystal (left), PDL02/DCF microparticles fabricated by Cryomilling (right).

second case (PGSS method), a pulse-periodic injection of SCF plasticized polymer/radical mixture through a nozzle into the receiving chamber at atmospheric pressure was performed. The product was kept under atmospheric conditions for 3 h (the time required for complete removal of CO_2 from the polymer particles), and then was blown with nitrogen at pressure of 0.4 - 0.5 MPa in order to spray out the resulting agglomerates of polymer microparticles. The obtained polymer microparticles, doped with paramagnetic substance, were placed in sealed plastic tubes and stored at room temperature.

The surface morphology of the particles was studied by scanning electron microscopy (SEM) on an LEO 1450 microscope (Carl Zeiss, Germany). A small amount of the powder was applied onto a conductive (carbon) adhesive tape, which was then sprayed by thin ($\sim$ 0.02-0.05 μm) gold film, providing the required electrical conductivity.

2.3. EPR spectroscopy

The EPR measurements were performed by X-band spectrometer Bruker EMX-500. The temperature of the samples was set in the range 90-373 K using the flow of nitrogen. The temperature was regulated using a Bruker thermal set-up with an accuracy of $\pm$1 K. EPR spectra of dry polymer microcapsules ($\sim$0.02 g) were recorded in a standard quartz ampule for EPR measurements with inner diameter of 3 mm. EPR spectra of aqueous solutions of param-

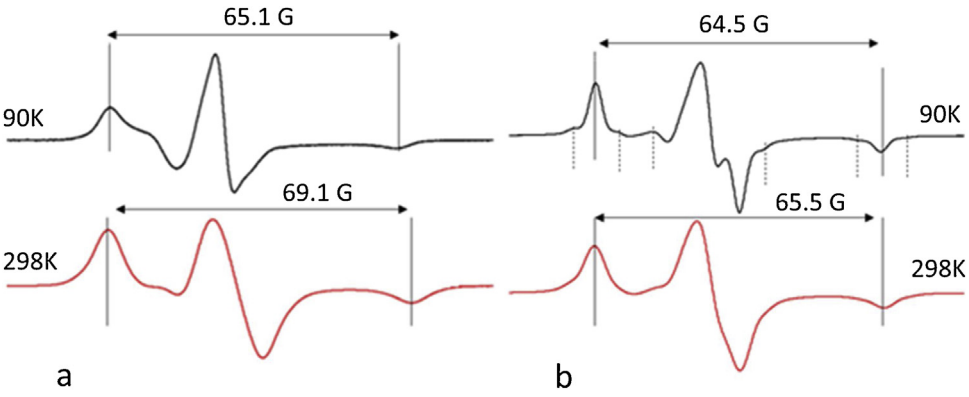

Fig. 6. EPR spectra of TEMPOL (a) and ATI (b) in PDL02.

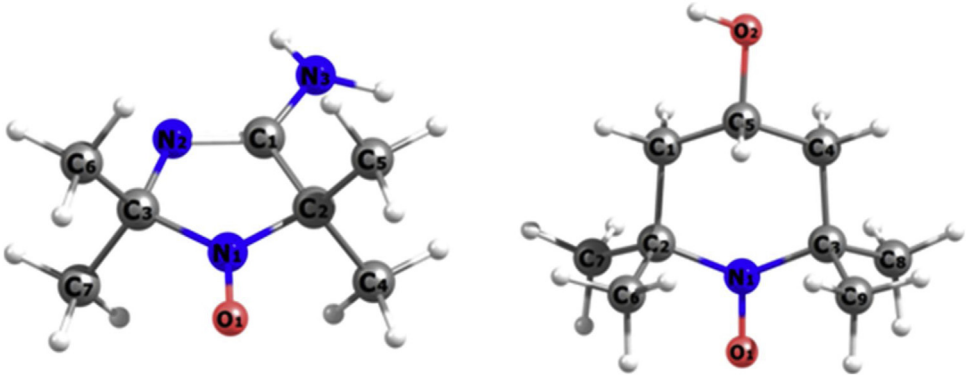

Fig. 7. Optimized structures of ATI (left) and TEMPOL (right).

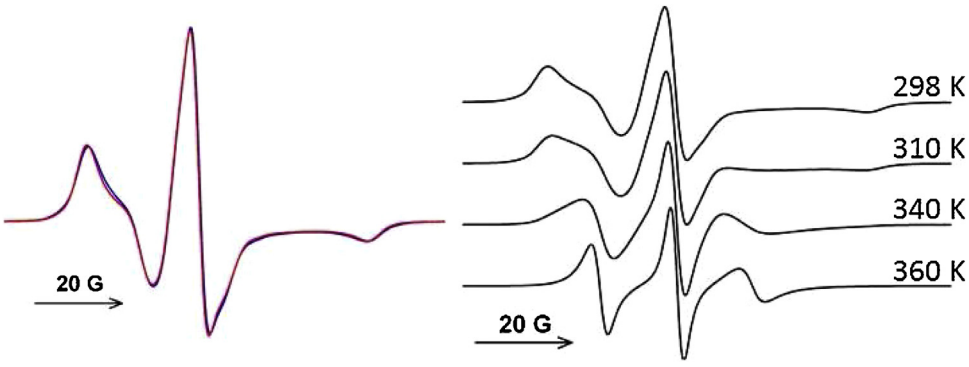

Fig. 8. EPR spectra of TEMPOL in PDL02 recorded immediately after SCF impregnation (red line) and after one year of storage of the sample at room temperature (blue line) (left); temperature dependence of the spectra (right).

agnetic substances or mixtures of aqueous solutions with swollen polymers were recorded in glass capillaries with inner diameter of 1.6 mm, the height of the sample was less than 3–4 mm.

The number of paramagnetic molecules in the dry samples was determined by standard method of EPR spectra double integration. The minute amount of nitroxide radicals in aqueous solutions (10^{12} - 10^{13} molecules) was determined by the method based on convolution of a highly noisy spectrum with the standard spectrum [47]. Estimation of local concentrations of the spin probes was carried out according to the method using the empirical parameter characterizing the shape of the EPR spectrum recorded in the absence of the rotational mobility of paramagnetic molecules (at the rigid limit) [22].

The processes of polymer swelling in sc–CO_2 and release of carbon dioxide from the polymer during decrease of pressure and temperature to ambient conditions are not equilibrium. In this case uneven distribution of the dopant over the sample is possible. In the case when paramagnetic molecules are concentrated in a small volume of a polymer, the EPR spectrum can be significantly broadened due to dipole-dipole interaction. The width of the spectral line may be so large that it may merge with background and, thus, some of the particles become “invisible” in the EPR spectrum. To avoid the errors associated with the described effect the impregnated polymer microparticles were dissolved in toluene and concentration of paramagnetic substance in the solution was determined using double integration of the spectra. It was found that the quantity of paramagnetic molecules in a dry polymer and in solution coincides, that is, no regions of locally concentrated paramagnetic molecules exist in the polymer matrix.

Table 1
Hfc constants on ^{13}C for ATI and TEMPOL (B3LYP/N07D).

ATI	C2	C3	C4	C5	C6	C7
A_{iso}, G	7.3	6.2	7.6	7.6	5.8	5.6
TEMPOL	C2	C3	C6	C7	C8	C9
A_{iso}, G	4.1	4.1	6.5	2.9	2.9	6.5

2.4. In vitro *paramagnetics release*

0.1 g of polymer microparticles and 2 mL of phosphate-buffered saline (PBS) were mixed in 8 mL vial and kept in the orbital shaker-incubator ES-20 (Biosan, Latvia) at 310 K. The solution was replaced every 2 days for preventing a pH decrease of the medium due to hydrolysis of polylactide. Every two hours on the first day and every 1–2 days on subsequent days 5–10 μg of the solution were taken for measuring the amount of paramagnetic particles by EPR.

EPR spectra of paramagnetic molecules in the polymer particles swollen in PBS solution were obtained as follows. Every 1–3 days the solution was removed from the vial, and particles were washed by new portions of PBS until the absence of paramagnetic particles in the solution was observed. Then EPR spectrum of cleaned particles was recorded.

To study the processes of the polymer swelling and dopant release, 1–2 mg of the doped polymer and 8–10 μL of PBS were placed into 1.6 mm glass ampoule, which was hereafter sealed. The EPR spectra of the sample were recorded at 310 K during several hours. Further, the sample was placed in a shaker at 310 K, and the spectra were recorded every two days at ambient conditions.

2.5. *Quantum chemical calculations*

Quantum chemical calculations were performed using ORCA 3.0.3 program package [48]. Geometries of ATI and TEMPOL were optimized on UKS/B3LYP/6–31 G(d,p) level [49]. Frequency analysis was carried out to confirm that optimized structures are minima on potential energy surface. N07D basis set [50] was used for calculations of hyperfine structure tensors.

3. Results and discussion

3.1. *Scanning electron microscopy*

Typical SEM images of initial paramagnetic compounds and their various PDL02/paramagnetics composite fabricated by SCF plasticization and foaming followed by Cryomilling and by PGSS technique are shown in Figs. 3–5.

3.2. *Content and localization of paramagnetic dopants in polymer microparticles*

The EPR spectra of TEMPOL, DHQ, TCF, DCF, and ATI radicals in PDL02 recorded at 90 K and 298 K are broad and asymmetric (Fig. 6). The distances between the lateral components of the spectra recorded at ambient conditions are typical for frozen motion of paramagnetic molecules due to glassy state of the polymer [51].

The spectra of the samples produced by PGSS and Cryomilling are similar. It is well-known that the shape of EPR spectra of radicals in a polymer matrix is very sensitive to the local environment of paramagnetic molecules [22]. Thus, the local environment of radicals in PDL02 does not depend on the obtaining procedure. The EPR spectra of all PDL02/paramagnetics composite microparticles do not change during one year of storage of the samples at room temperature manifesting that local environment of paramagnetic molecules does not change over time (Fig. 8).

Room-temperature EPR spectra of ATI and DCF contain additional components (marked with dotted lines in Fig. 6b). The same shape of spectra of radicals including nitroxide fragment with five-membered cycle was observed previously [52]. We suggest that the additional components can be manifested due to hyperfine interaction of the unpaired electron with ^{13}C atoms located nearby the NO group. To test this hypothesis, ^{13}C hyperfine coupling (hfc) isotropic constants of ATI and TEMPOL were calculated using DFT method. In the case of ATI the constants values for carbon atoms bonded with the nitrogen atom of the NO fragment and carbon atoms of four methyl groups are within the range of 5.6 G to 7.6 G (Table 1). The corresponding constants of TEMPOL are smaller (2.9 G – 6.5 G). Thus, the presence of the side components in the EPR spectra of five-membered nitroxide radicals, apparently, is due to hfc on ^{13}C nuclei (Fig. 7).

To study the changes of mobility of the polymer chains, a series of EPR spectra of the PDL02/paramagnetics composite microparticles were recorded in the temperature range 298–360 K (TEMPOL spectra as an example are presented in Fig. 8). The line shape changes dramatically with increasing temperature: broad anisotropic spectrum of slow-moving particles gradually changes to a wide triplet of rotating radicals. This fact evidences an increase of the segmental mobility of the polymer chains. EPR spectra recorded at the same temperatures during heating and cooling of the samples almost coincide. Hence, reversible relaxation of the polymer matrix takes place. The behavior of samples made by Cryomilling and PGSS does not differ.

EPR spectra recorded at 90 K were simulated using ODF3 program [53]. Only hyperfine interaction of the unpaired electron with the ^{14}N nucleus was considered. The direction of the main axes of the hfc tensor was assumed to coincide with the direction of the g-tensor main axes. The shape of the individual resonance line was represented as a convolution of the Gaussian and Lorentz functions. As an example, Fig. 9 shows the result of simulation of the spectra

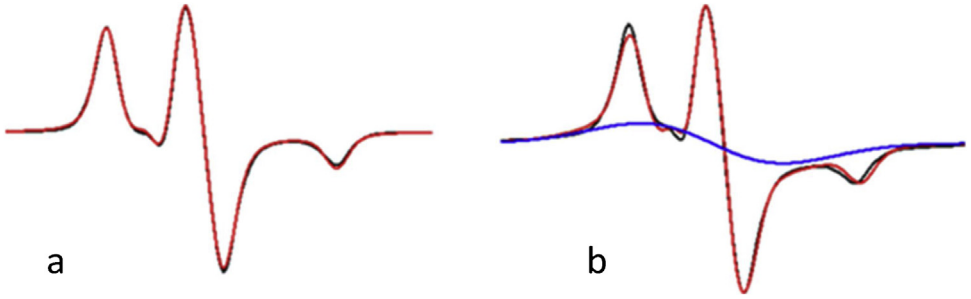

Fig. 9. EPR spectra of TEMPOL (a) and DHQ (b) and results of their simulation. Black lines – experimental spectra, red lines – results of simulation, blue line – signal of magnetically concentrated radicals (see text).

Table 2
Spin-Hamiltonian parameters of paramagnetic substances in polymer matrixes.

radical/ polymer or solvent	g_{xx} ±0.0002	g_{yy} ±0.0002	g_{zz} ±0.0002	A_{xx} ±0.2 G	A_{yy} ±0.2 G	A_{zz} ±0.05 G
TEMPOL /methanol[a]	2.0090	2.0061	2.0022	–	7.3	37.0
TEMPOL/ Toluene[a]	2.0099	2.0063	2.0022	6.2	7.0	34.3
TEMPOL/ PDLLA	2.0098	2.0066	2.0024	7.2	5.7	34.3
DHQ/ PDLLA	2.0096	2.0061	2.0022	4.5	4.6	34.4
DCF/ PDLLA	2.0099	2.0067	2.0024	5.6	4.5	34.6
TCP/ PDLLA	2.0096	2.0063	2.0021	7.0	5.6	34.0
ATI/ PDLLA	2.0094	2.0066	2.0024	4.6	4.0	32.6

[a] [54].

Table 3
Concentration of the paramagnetic substances in PDLLA microparticles.

Radical/impregnation technique	Concentration, mmol/g
TEMPOL/CM	0.27 ± 0.04
TEMPOL/PGSS	0.33 ± 0.05
DCF/PGSS	0.43 ± 0.06
DHQ/PGSS	0.04 ± 0.01
TCP/PGSS	0.22 ± 0.03
ATI/PGSS	0.82 ± 0.12

of TEMPOL and DHQ in PDLLA. The spectrum of DHQ is the sum of the standard spectrum of nitroxide radical and a wide unstructured singlet which indicates the presence of regions with high local concentration of paramagnetic substances. Contribution of the singlet line to the integral intensity of the spectrum comes to ~40 %. Concentration of spin labeled dihydroquercetin may be due to its poor solubility in the polymer plasticized in $scCO_2$.

Spin-Hamiltonian parameters of the paramagnetic molecules in polymer matrixes, which were determined as a result of the spectra simulation, are presented in Table 2. For comparison, Table 2 also contains the principle values of the g-tensor and the hfc tensor of TEMPOL in toluene (non-polar solvent) and methanol (polar solvent). It is known that g_{xx} and A_{zz} are very sensitive to the polarity of local environment of nitroxide radicals. Comparing literature values and the data presented in this paper, one can conclude that paramagnetic substances are predominantly located in non-polar environment.

The concentrations of nitroxides in the polymer microparticles are presented in Table 3. In all cases, except for DHQ, the content is approximately 10^{-4} mol per gram of the polymer; thereby the mass fraction of the radicals is about 0.01 %. The concentration of DHQ is an order of magnitude lower. This result confirms that spin labeled dihydroquercetin is poorly soluble in PDL02 plasticized by $sc{-}CO_2$.

3.3. *Kinetic peculiarities of paramagnetic compounds release from polymer microparticles in PBS*

Kinetic curves of TEMPOL and DCF release from polylactide microparticles (produced by PGSS) to PBS are presented in Fig. 10. In the case of small molecules TEMPOL, the triphasic profile typical for release from macromolecular drug delivery systems is observed [55]. A significant fraction of the paramagnetic substance leaves the polymer matrix during first 5 days. The initial fast release of the dopant, so-called "initial burst", was observed by many researchers [21,55–58], just to mention a few. The rapid release typically accounts for 10–80 % of the total dopant loading. When polymer

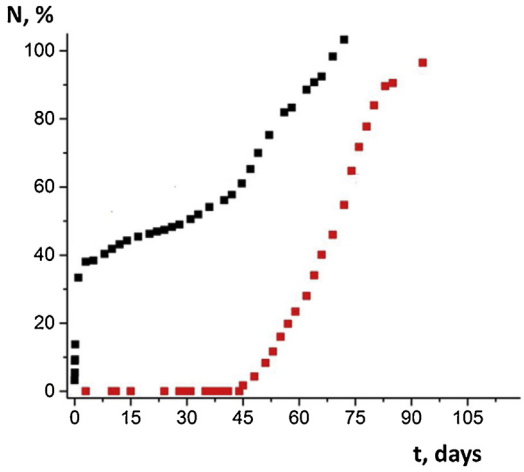

Fig. 10. Kinetic plots of the release of TEMPOL (black symbols) and DCF (red symbols) from PDL02 microparticles into PBS.

particles are used for biomedical purposes, this phenomenon poses a serious problem dealing with excess of toxic level in vivo and is a major hurdle for the development of microparticle products [56]. The burst is associated with dissolution of dopant from the microparticle surface [55], heterogeneous distribution of dopant in the polymer matrix [21], fast swelling of thin walls of near-surface pores [56]. After 5 days of immersion the lag stage begins, during which the dopant diffuses slowly either through the relatively dense polymer or through the existing pores, while polymer swelling and degradation proceed in the bulk [55,57,58]. Approximately on 45th day the perceptible acceleration attributed to the onset of essential polymer erosion and degradation [57,59].

At the same time, DCF release curves are characterized by long induction period. The release of DCF begins simultaneously with the polymer erosion corresponding to the third stage of TEMPOL release.

The data of a dopant release kinetics from the polymer to the external media can be collected by UV spectroscopy [18], high performance liquid chromatography [60], with the use of special reagents [61], etc. However, these methods don't allow determining the localization of the dopant molecules inside the polymer structure at various stages of swelling and degradation of the matrix. Such information is of great interest because it can clarify the mechanism of the dopant diffusion through the polymer matrix containing the pores filled by liquid. EPR spectroscopy permits simultaneously analyzing as release kinetics and the localization of the paramagnetic molecules inside the polymer.

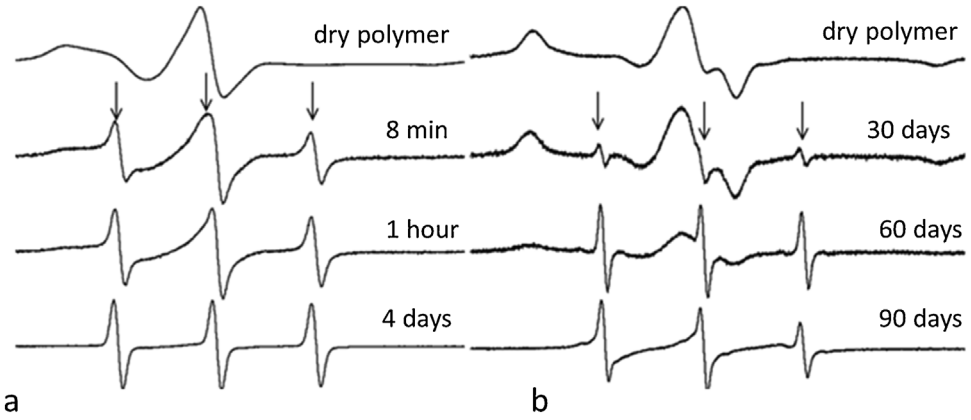

Fig. 11. EPR spectra of a mixture of polymer particles impregnated with TEMPOL (a) and DCF (b) and a buffer solution.

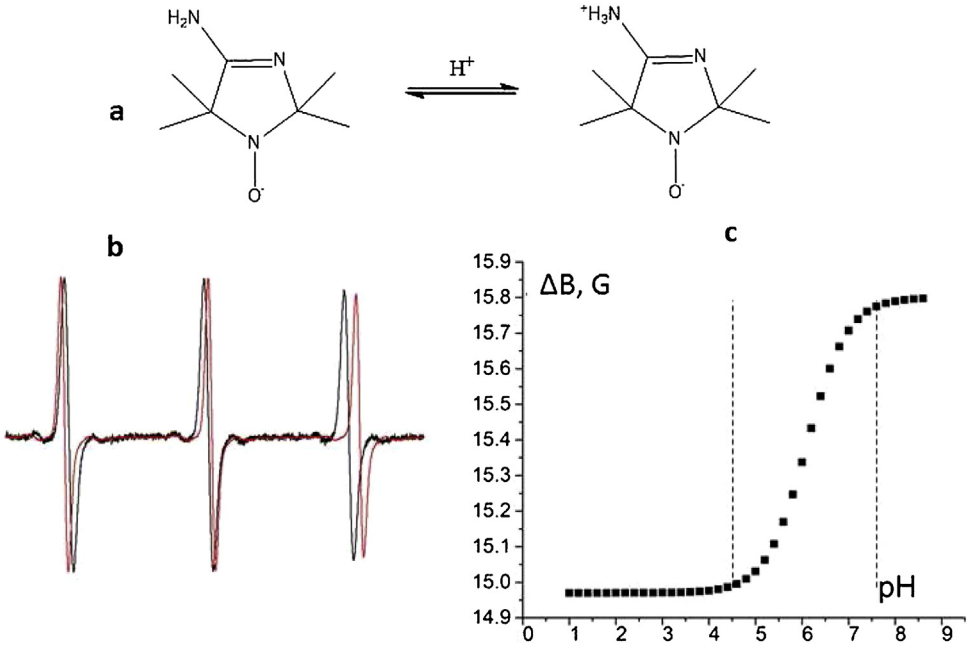

Fig. 12. Protolytic equilibrium of the ATI radical (a), EPR spectra of the protonated (black) and non-protonated (red) forms of ATI in aqueous solution (b), dependence of the distance between left and central components of EPR spectrum of ATI radical in aqueous solution on pH (c).

To determine the localization of paramagnetic molecules inside the water absorbed polymer sample, the EPR spectra of a mixture of PDL02/paramagnetics composite microparticles and a buffer solution were recorded. The results are shown in Fig. 11. It can be seen that over time the three narrow components appear in the spectra on the background of the signal of the radicals in the polymer matrix. The narrow triplet is uniquely associated with the radicals with high rotational mobility. Obviously these paramagnetic molecules are localized in non-viscous, that is, in an aqueous medium. Such radicals have either already left the microparticles, or are in the water-accessible regions of the sample but are not localized inside the polymer matrix. In the case of the TEMPOL in 8 min after immersion of the polymer in the buffer solution a significant content of mobile molecules is observed, which continues to grow over time. In 4 days the spectrum of the low mobile radicals inside the polymer is no longer distinguishable. In the case of DCF the content of mobile molecules remains very small for a long time (~30 days). This suggests that during the swelling of the microparticles the radicals remain inside the polymer matrix and don't release into the pores. After beginning the polymer erosion the number of fast moving DCF molecules increases rapidly. The complete absence of the release of spin labeled diclofenac from PDL02 into the external solution up to 45 days may be due to large size of DCF molecules as well as due to specific interactions of this substance with polylactide molecules.

Hydrolytic decomposition of PDL02 is accompanied by the formation of acid, which can lead to a significant decrease in pH inside the polymer sample [62,13]. Many drug compounds are unstable in an acidic medium [63–65], so the issue of estimating changes in the local pH inside the polymer matrix during hydrolysis is of great importance. In the present work for this aim the pH-sensitive spin probe ATI which can exist in protonated and non-protonated forms was used (Fig. 12a). Fig. 12b shows the EPR spectra of the protonated and non-protonated forms of ATI. It can be seen that the distances between the components of these spectra are different; the maximum difference is observed between the positions of the right components. From the analysis of the presented spectra, the average values of the g factor and the hfc constants for the protonated and non-protonated forms of ATI were obtained. Based on the literary pK_a value a calibration curve was constructed for the radical used (Fig. 12c). It can be seen that the ATI radical is sensitive to changes in pH in the range 4.5–7.5.

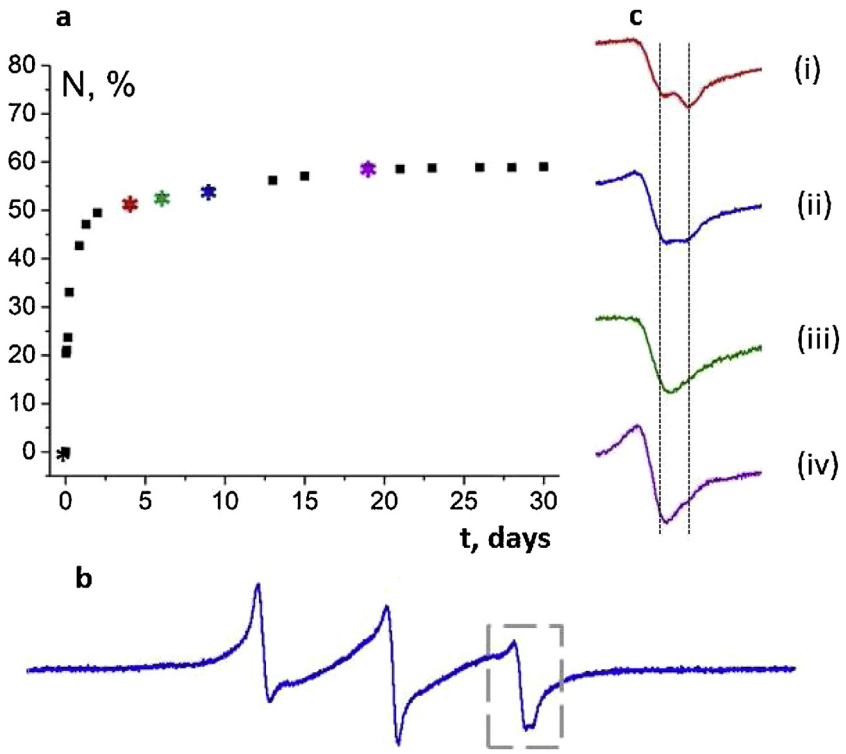

Fig. 13. Kinetic plot of ATI release from PDL02 microparticles into PBS (a), typical shape of EPR spectrum of ATI in swelled microparticles (b) and EPR spectra fragments of the microparticles extracted from the buffer solution at different time points (c): after 5 days (i), 7 days (ii), 9 days (iii) and 19 days (iv) of exposure.

The typical EPR spectrum of swollen microparticles impregnated with ATI is shown in Fig. 13b. The spectra of swollen particles are the sum of several triplet spectra differing in line width and corresponding to radicals with high rotational mobility. It can be seen that the high field component of the spectra is split into two lines corresponding to protonated and non-protonated forms of ATI (in Figure these components are marked with dotted lines). The change of the right spectral component shape during the polymer swelling (Fig. 13c) indicates that the amount of non-protonated form decreases and the amount of protonated one increases. In 9 days after the immersion of the particles into solution the line corresponding to non-protonated form was no longer distinguishable in the spectrum, that is, the pH inside the particles changed to a value less than 4.5. On the radical release curve at that time there was the stagnation stage. So, there is a significant decrease in pH inside the PDL02 microparticles when about half of the dopant is still in the sample. This circumstance must be taken into account when medicinal substances sensitive to the acidity of the medium are introduced into microparticles of PDL02.

4. Conclusions

It was shown experimentally that SCF techniques enabling fabrication of poly(D,L-lactide) microparticles, comprising their simultaneous impregnation with different low molecular weight paramagnetic compounds and providing a certain spatial distribution of encapsulated substances. EPR spectroscopy did not reveal any irreversible relaxation processes in the polymer structures and bioactive formulations produced. The difference in kinetic peculiarities of the release of a small TEMPOL and larger DCF molecules from micronized poly(D,L-lactide) in PBS was observed. It was revealed using ATI pH-sensitive spin probe that local pH inside the microparticles decreases to pH $\leq$ 4.5 during the first 9 days after their immersion into a buffer solution. These results can be useful and applicable for research and development of a new control release drug formulation and components based upon biodegradable aliphatic polyesters.

Declaration of Competing Interest

No potential conflict of interest was reported by the authors

Acknowledgments

This work was supported by the Ministry of Science and Higher Education within the State assignment FSRC «Crystallography and Photonics» RAS in part of SCF encapsulation of paramagnetic compounds in biodegradable polymer particles and by Russian Foundation for Basic Research (grants 17-02-00445 and 18-29-06059) in part of EPR investigation and Russian Science Foundation grant 19-13-00235 in part of spin probes synthesis. The synthesis of DCF was financed by the Higher Education Institutional Excellence Programme of the Ministry for Innovation and Technology in Hungary, within the framework of the TUDFO/47138/2019-ITM thematic programme of the Pécs University. The authors acknowledge support from M.V. Lomonosov Moscow State University Program of Development.

References

[1] J.M. Anderson, M.S. Shive, Biodegradation and biocompatibility of PLA and PLGA microspheres, Adv. Drug Deliv. Rev. 64 (2012) 72–82, http://dx.doi.org/10.1016/j.addr.2012.09.004.
[2] K. Mishima, Biodegradable particle formation for drug and gene delivery using supercritical fluid and dense gas, Adv. Drug Deliv. Rev. 60 (2008) 411–432, http://dx.doi.org/10.1016/j.addr.2007.02.003.
[3] R. Tong, N.P. Gabrielson, T.M. Fan, J. Cheng, Polymeric nanomedicines based on poly (lactide) and poly (lactide-co-glycolide), Curr. Opin. Solid State Mater. Sci. 16 (2013) 323–332.
[4] S.K. Shukla, S.K. Shukla, P.P. Govender, N.G. Giri, Biodegradable polymeric nanostructures in therapeutic applications: opportunities and challenges, RSC Adv. 6 (2016) 94325–94351, http://dx.doi.org/10.1039/c6ra15764e.

[5] J. Panyam, V. Labhasetwar, Biodegradable nanoparticles for drug and gene delivery to cells and tissue, Adv. Drug Deliv. Rev. 64 (2012) 61–71, http://dx.doi.org/10.1016/j.addr.2012.09.023.
[6] A. Martín, M.J. Cocero, Micronization processes with supercritical fluids: fundamentals and mechanisms, Adv. Drug Deliv. Rev. 60 (2008) 339–350, http://dx.doi.org/10.1016/j.addr.2007.06.019.
[7] W.L. Priamo, I. Dalmolin, D.L. Boschetto, N. Mezzomo, S.R.S. Ferreira, J.V. Oliveira, Processos de micronização utilizando tecnologia supercrítica: uma breve revisão sobre projeto de processos (200-2012), Acta Sci. Pol. Technol. Aliment. 35 (2013) 695–709, http://dx.doi.org/10.4025/actascitechnol.v35i4.18819.
[8] C. Wischke, S.P. Schwendeman, Principles of encapsulating hydrophobic drugs in PLA/PLGA microparticles, Int. J. Pharm. 364 (2008) 298–327, http://dx.doi.org/10.1016/j.ijpharm.2008.04.042.
[9] S.M. Howdle, M.S. Watson, M.J. Whitaker, V.K. Popov, M.C. Davies, F.S. Mandel, J.D. Wang, K.M. Shakesheff, Supercritical fluid mixing: preparation of thermally sensitive polymer composites containing bioactive materials, Chem. Commun. (Camb.) (2001) 109–110, http://dx.doi.org/10.1039/b008188o.
[10] H. Tai, V.K. Popov, K.M. Shakesheff, S.M. Howdle, Putting the fizz into chemistry: applications of supercritical carbon dioxide in tissue engineering, drug delivery and synthesis of novel block copolymers, Biochem. Soc. Trans. 35 (2007) 516–521, http://dx.doi.org/10.1042/BST0350516.
[11] C.S. Proikakis, N.J. Mamouzelos, P.A. Tarantili, A.G. Andreopoulos, Swelling and hydrolytic degradation of poly(d,l-lactic acid) in aqueous solutions, Polym. Degrad. Stab. 91 (2006) 614–619, http://dx.doi.org/10.1016/j.polymdegradstab.2005.01.060.
[12] A.G. Andreopoulos, E. Hatzi, M. Doxastakis, Controlled release of salicylic acid from poly(D,L-Lactide), J. Mater. Sci. Mater. Med. 12 (2001) 233–239, http://dx.doi.org/10.1023/A:1008911131657.
[13] A. Brunner, K. Mader, A. Gopferich, pH and osmotic pressure inside biodegradable microspheres during erosion, Pharm. Res. 16 (1999) 847–853, http://dx.doi.org/10.1023/A:1018822002353.
[14] P.I. Borovikov, A.P. Sviridov, E.N. Antonov, A.G. Dunaev, L.I. Krotova, T.K. Fatkhudinov, V.K. Popov, Model of aliphatic polyesters hydrolysis comprising water and oligomers diffusion, Polym. Degrad. Stab. 159 (2019) 70–78, http://dx.doi.org/10.1016/j.polymdegradstab.2018.11.017.
[15] K. Mäder, B. Gallez, K.J. Liu, H.M. Swartz, Non-invasive in vivo characterization of release processes in biodegradable polymers by low-frequency electron paramagnetic resonance spectroscopy, Biomaterials 17 (1996) 457–461, http://dx.doi.org/10.1016/0142-9612(96)89664-5.
[16] M. Dunne, O.I. Corrigan, Z. Ramtoola, Influence of particle size and dissolution conditions on the degradation properties of polylactide-co-glycolide particles, Biomaterials 21 (2000) 1659–1668, http://dx.doi.org/10.1016/S0142-9612(00)00040-5.
[17] K. Sevim, J. Pan, A mechanistic model for acidic drug release using microspheres made of PLGA 50:50, Mol. Pharm. 13 (2016) 2729–2735, http://dx.doi.org/10.1021/acs.molpharmaceut.6b00313.
[18] D. Klose, F. Siepmann, K. Elkharraz, J. Siepmann, PLGA-based drug delivery systems: importance of the type of drug and device geometry, Int. J. Pharm. 354 (2008) 95–103, http://dx.doi.org/10.1016/j.ijpharm.2007.10.030.
[19] E.N. Antonov, A.G. Dunaev, S.A. Minaeva, L.I. Krotova, V.K. Popov, Effects of pharmaceutical preparations on the rate of degradation of poly(Lactide-Co-Glycolide) scaffolds, Pharm. Chem. J. 52 (2018) 69–76, http://dx.doi.org/10.1007/s11094-018-1767-8.
[20] H.V. Maulding, T.R. Tice, D.R. Cowsar, J.W. Fong, J.E. Pearson, J.P. Nazareno, Biodegradable microcapsules: acceleration of polymeric excipient hydrolytic rate by incorporation of a basic medicament, J. Control. Release 3 (1986) 103–117, http://dx.doi.org/10.1016/0168-3659(86)90071-4.
[21] X. Huang, C.S. Brazel, On the importance and mechanisms of burst release in matrix-controlled drug delivery systems, J. Control. Release 73 (2001) 121–136, http://dx.doi.org/10.1016/S0168-3659(01)00248-6.
[22] A.I. Kokorin, Nitroxides - Theory, Experiment and Application, InTech, Rijeka, 2012, 436 p.
[23] G. Karthikeyan, A. Bonucci, G. Casano, G. Gerbaud, S. Abel, V. Thomé, L. Kodjabachian, A. Magalon, B. Guigliarelli, V. Belle, O. Ouari, E. Mileo, A bioresistant nitroxide spin label for in-cell EPR spectroscopy: in vitro and in oocytes protein structural dynamics studies, Angew. Chemie - Int. Ed. 57 (2018) 1366–1370, http://dx.doi.org/10.1002/anie.201710184.
[24] A. Nalepa, K. Möbius, M. Plato, W. Lubitz, A. Savitsky, Nitroxide spin labels—magnetic parameters and hydrogen-bond formation: a high-field EPR and EDNMR study, Appl. Magn. Reson. 50 (2019) 1–16, http://dx.doi.org/10.1007/s00723-018-1073-3.
[25] A. Matsumoto, Y. Matsukawa, Y. Horikiri, T. Suzuki, Rupture and drug release characteristics of multi-reservoir type microspheres with poly(dl-lactide-co-glycolide) and poly(dl-lactide), Int. J. Pharm. 327 (2006) 110–116, http://dx.doi.org/10.1016/j.ijpharm.2006.07.055.
[26] P.K. Chatterjee, S. Cuzzocrea, P.A.J. Brown, K. Zacharowski, K.N. Stewart, H. Mota-Filipe, C. Thiemermann, Tempol, a membrane-permeable radical scavenger, reduces oxidant stress-mediated renal dysfunction and injury in the rat, Kidney Int. 58 (2000) 658–673, http://dx.doi.org/10.1046/j.1523-1755.2000.00212.x.
[27] M. Isbera, B. Bognár, G. Gulyás-Fekete, K. Kish, T. Kálai, Syntheses of pyrazine-, quinoxaline-, and imidazole-fused pyrroline nitroxides, Synthesis (Stuttg) (2019), http://dx.doi.org/10.1055/s-0039-1690678.
[28] B. Bognár, G. Úr, C. Sár, O.H. Hankovszky, K. Hideg, T. Kálai, Synthesis and application of stable nitroxide free radicals fused with Carbocycles and heterocycles, Curr. Org. Chem. 23 (2019) 480–501, http://dx.doi.org/10.2174/1385272823666190318163321.
[29] I.A. Grigor'ev, N.I. Tkacheva, S.V. Morozov, Conjugates of natural compounds with nitroxyl radicals as a basis for creation of pharmacological agents of new generation, Curr. Med. Chem. 21 (2014) 2839–2852, http://dx.doi.org/10.2174/0929867321666140304153104.
[30] Q.M. Andersen, Flavonoids: Chemistry, Biochemistry and Applications, CRC Press, 2006.
[31] A.E. Weidmann, Dihydroquercetin: More than just an impurity? Eur. J. Pharmacol. 684 (2012) 19–26, http://dx.doi.org/10.1016/j.ejphar.2012.03.035.
[32] L.I. Cabezas, I. Gracia, M.T. García, A. De Lucas, J.F. Rodríguez, Production of biodegradable porous scaffolds impregnated with 5-fluorouracil in supercritical CO2, J. Supercrit. Fluids 80 (2013) 1–8, http://dx.doi.org/10.1016/j.supflu.2013.03.030.
[33] K.N. Engin, Alpha-tocopherol: looking beyond an antioxidant, Mol. Vis. 15 (2009) 855–860.
[34] Y.V. Yushkova, E.I. Chernyak, S.V. Morozov, I.A. Grigor'ev, First spin-labeled α-tocopherol and trolox succinyl derivatives, Chem. Nat. Compd. 50 (2014) 827–831, http://dx.doi.org/10.1007/s10600-014-1093-7.
[35] O.D. Zakharova, T.S. Frolova, Y.V. Yushkova, E.I. Chernyak, A.G. Pokrovsky, M.A. Pokrovsky, S.V. Morozov, O.I. Sinitsina, I.A. Grigor'ev, G.A. Nevinsky, Antioxidant and antitumor activity of trolox, trolox succinate, and α-tocopheryl succinate conjugates with nitroxides, Eur. J. Med. Chem. 122 (2016) 127–137, http://dx.doi.org/10.1016/j.ejmech.2016.05.051.
[36] T. Yamazaki, M. Muramoto, T. Oe, N. Morikawa, O. Okitsu, T. Nagashima, S. Nishimura, Y. Katayama, Y. Kita, Diclofenac, a non-steroidal anti-inflammatory drug, suppresses apoptosis induced by endoplasmic reticulum stresses by inhibiting caspase signaling, Neuropharmacology 50 (2006) 558–567, http://dx.doi.org/10.1016/j.neuropharm.2005.10.016.
[37] M. Tunçay, S. Çaliş, H.S. Kaş, M.T. Ercan, I. Peksoy, A.A. Hincal, Diclofenac sodium incorporated PLGA (50:50) microspheres: formulation considerations and in vitro/in vivo evaluation, Int. J. Pharm. 195 (2000) 179–188, http://dx.doi.org/10.1016/S0378-5173(99)00394-4.
[38] S.S. Guterres, H. Fessi, G. Barratt, J.P. Devissaguet, F. Puisieux, Poly (DL-lactide) nanocapsules containing diclofenac: I. Formulation and stability study, Int. J. Pharm. 113 (1995) 57–63, http://dx.doi.org/10.1016/0378-5173(94)00177-7.
[39] A.A. Barba, A. Dalmoro, M. D'Amore, C. Vascello, G. Lamberti, Biocompatible nano-micro-particles by solvent evaporation from multiple emulsions technique, J. Mater. Sci. 49 (2014) 5160–5170, http://dx.doi.org/10.1007/s10853-014-8224-1.
[40] P. Scarfato, E. Avallone, M.R. Galdi, L. Di Maio, L. Incarnato, Preparation, characterization, and oxygen scavenging capacity of biodegradable α-tocopherol/PLA microparticles for active food packaging applications, Polym. Compos. 38 (2017) 981–986, http://dx.doi.org/10.1002/pc.23661.
[41] G. Della Porta, N. Falco, E. Reverchon, NSAID drugs release from injectable microspheres produced by supercritical fluid emulsion extraction, J. Pharm. Sci. 99 (2010) 1484–1499, http://dx.doi.org/10.1002/jps.21920.
[42] V.V. Khramtsov, L.M. Weiner, I.A. Grigoriev, L.B. Volodarsky, Proton exchange in stable nitroxyl radicals, EPR study of the pH of aqueous solutions, Chem. Phys. Lett. 91 (1982) 69–72, http://dx.doi.org/10.1016/0009-2614(82)87035-8.
[43] N.V. Kosheleva, E.I. Chernyak, Y.F. Polienko, S.V. Morozov, I.A. Grigor'ev, Use of the mannich reaction to synthesize spin-labeled derivatives of the natural flavonoid dihydroquercetin, Chem. Nat. Compd. 50 (2014) 261–265, http://dx.doi.org/10.1007/s10600-014-0927-7.
[44] H.O. Hankovszky, K. Hideg, L. Lex, Nitroxyls; VII 1. Synthesis and reactions of highly reactive 1-Oxyl-2,2,5,5-tetramethyl-2,5-dihydropyrrole-3-ylmethyl sulfonates, Synthesis (Stuttg 1980 (1980) 914–916, http://dx.doi.org/10.1055/s-1980-29269.
[45] I. Pasquali, R. Bettini, F. Giordano, Supercritical fluid technologies: an innovative approach for manipulating the solid-state of pharmaceuticals, Adv. Drug Deliv. Rev. 60 (2008) 399–410, http://dx.doi.org/10.1016/j.addr.2007.08.030.
[46] I. Kikic, Polymer–supercritical fluid interactions, J. Supercrit. Fluids 47 (2009) 458–465, http://dx.doi.org/10.1016/j.supflu.2008.10.016.
[47] N.A. Chumakova, S.V. Kuzin, A.I. Grechishnikov, Spectral convolution for quantitative analysis in EPR spectroscopy, Appl. Magn. Reson. 50 (2019) 1125–1147, http://dx.doi.org/10.1007/s00723-019-01133-9.
[48] F. Neese, The ORCA program system, Wiley Interdiscip, Rev. Comput. Mol. Sci. 2 (2012) 73–78, http://dx.doi.org/10.1002/wcms.81.
[49] W.J. Hehre, K. Ditchfield, J.A. Pople, Self-consistent molecular orbital methods. XII. Further extensions of gaussian-type basis sets for use in molecular orbital studies of organic molecules, J. Chem. Phys. 56 (1972) 2257–2261, http://dx.doi.org/10.1063/1.1677527.
[50] V. Barone, P. Cimino, E. Stendardo, Development and validation of the B3LYP/N07D computational model for structural parameter and magnetic tensors of large free radicals, J. Chem. Theory Comput. 4 (2008) 751–764, http://dx.doi.org/10.1021/ct800034c.
[51] W. John, Electron Spin Resonance: Elementary Theory and Practical Applications, Chapman an, New York, 1986.
[52] D.A. Chernova, A.K. Vorobiev, Temperature dependence of ESR spectra of nitroxide spin probe in glassy polymers, J. Polym. Sci. Part B: Polym. Phys. 47 (2009) 563–575, http://dx.doi.org/10.1002/polb.21662.

[53] A.K. Vorobiev, N.A. Chumakova, Simulation of Rigid-Limit and Slow-Motion EPR Spectra for Extraction of Quantitative Dynamic and Orientational Information, 2012.
[54] R.I. Zhdanov, Bioactive spin labels, Gen. Pharmacol. Vasc. Syst. 24 (1993) 1293, http://dx.doi.org/10.1016/0306-3623(93)90394-D.
[55] N. Kamaly, B. Yameen, J. Wu, O.C. Farokhzad, Degradable controlled-release polymers and polymeric nanoparticles: mechanisms of controlling drug release, Chem. Rev. 116 (2016) 2602–2663, http://dx.doi.org/10.1021/acs.chemrev.5b00346.
[56] J. Wang, B.M. Wang, S.P. Schwendeman, Characterization of the initial burst release of a model peptide from poly(D,L-lactide-co-glycolide) microspheres, J. Control. Release 82 (2002) 289–307, http://dx.doi.org/10.1016/S0168-3659(02)00137-2.
[57] S. Fredenberg, M. Wahlgren, M. Reslow, A. Axelsson, The mechanisms of drug release in poly(lactic-co-glycolic acid)-based drug delivery systems - A review, Int. J. Pharm. 415 (2011) 34–52, http://dx.doi.org/10.1016/j.ijpharm.2011.05.049.
[58] Y. Xu, C.S. Kim, D.M. Saylor, D. Koo, Polymer degradation and drug delivery in PLGA-based drug–polymer applications: a review of experiments and theories, J. Biomed. Mater. Res. - Part B Appl. Biomater. 105 (2017) 1692–1716, http://dx.doi.org/10.1002/jbm.b.33648.
[59] X. Pang, X. Zhuang, Z. Tang, X. Chen, Polylactic acid (PLA): research, development and industrialization, Biotechnol. J. (2010) 1125–1136, http://dx.doi.org/10.1002/biot.201000135.
[60] G.M. Xiao, W. L, Y. B, G, poly(Lactic acid)-Based biomaterials:synthesis,Modification and applications, Biomed. Sci. Eng. Technol. DN (Ed.). INTECH Publ. Rijeka, Croat. (2012) 247–282.
[61] M. Sandor, D. Enscore, P. Weston, E. Mathiowitz, Effect of protein molecular weight on release from micron-sized PLGA microspheres, J. Control. Release 76 (2001) 297–311, http://dx.doi.org/10.1016/S0168-3659(01)00446-1.
[62] K. Mäder, S. Nitschke, R. Stösser, H.H. Borchert, A. Domb, Non-destructive and localized assessment of acidic microenvironments inside biodegradable polyanhydrides by spectral spatial electron paramagnetic resonance imaging, Polymer (Guildf). 38 (1997) 4785–4794, http://dx.doi.org/10.1016/S0032-3861(97)00003-7.
[63] A. Schädlich, S. Kempe, K. Mäder, Non-invasive in vivo characterization of microclimate pH inside in situ forming PLGA implants using multispectral fluorescence imaging, J. Control. Release 179 (2014) 52–62, http://dx.doi.org/10.1016/j.jconrel.2014.01.024.
[64] E.A. Gadkariem, F. Belal, M.A. Abounassif, H.A. El-Obeid, K.E.E. Ibrahim, Stability studies on diloxanide furoate: effect of pH, temperature, gastric and intestinal fluids, Farmaco. 59 (2004) 323–329, http://dx.doi.org/10.1016/j.farmac.2003.11.015.
[65] M. Mathew, V. Das Gupta, R.E. Bailey, Stability of omeprazole solutions at various ph values as determined by high-performance liquid chromatography, Drug Dev. Ind. Pharm. 21 (1995) 965–971, http://dx.doi.org/10.3109/03639049509026660.